Adsorption and Corrosion inhibition of Azadirachta indica Gum with Zn2+/Ni2+ cations on Mild Steel in 1 mol L−1 HCl

Article *in* Oriental Journal of Chemistry · July 2015

DOI: 10.13005/ojc/310216

2 authors, including:

Brindha Thirumalairaj

8 PUBLICATIONS **112** CITATIONS

SEE PROFILE

Est. 1984

ORIENTAL JOURNAL OF CHEMISTRY
An International Open Free Access, Peer Reviewed Research Journal

www.orientjchem.org

ISSN: 0970-020 X
CODEN: OJCHEG
2015, Vol. 31, No. (2):
Pg. 741-752

Adsorption and Corrosion inhibition of *Azadirachta indica* Gum with Zn^{2+}/Ni^{2+} cations on Mild Steel in 1 mol L^{-1} HCl

T. BRINDHA and J. MALLIKA*

Department of Chemistry, PSG College of Arts and Science, Coimbatore - 641014, India.
*Corresponding author E-mail: jmpsgcas@gmail.com

http://dx.doi.org/10.13005/ojc/310216

(Received: March 26, 2015; Accepted: May 08, 2015)

ABSTRACT

This work deals with synergistic corrosion inhibition efficiency of *Azadirachta indica* gum and metal cations (Zn^{2+} and Ni^{2+}) on mild steel in 1 mol L^{-1} HCl using gravimetric, potentiodynamic polarization and electrochemical impedance spectroscopic methods. The effect of temperature (303 - 348± 1 K) and immersion time (1, 2, 3, 4, 6 and 24 h) on the inhibition of corrosion has also been studied. Corrosion kinetic parameters were calculated and discussed in detail. It obeys Langmuir adsorption isotherm. The interaction of inhibitors with the mild steel surface has been established by Fourier transform infrared spectroscopy.

Key words*:* mild steel, metal cations, corrosion inhibition, electrochemical techniques.

INTRODUCTION

The corrosion protection of mild steel is a significant concern among the corrosion scientist and material technologist[1]. Although, mild steel has remarkable economic and substantial applications, its poor corrosion resistance in acids confines its usage[2]. Acid solutions are widely used in pickling of steel, chemical cleaning/ processing, ore production and oil well acidification[3]. Several methods are used to control the corrosion process but application of inhibitors has been proven to be most practical and efficient for this purpose. Organic compounds containing nitrogen, sulphur and oxygen can be used as efficient corrosion inhibitors[4-6]. E.E. Oguzie *et al*.[7] observed that the presence of hetero-atoms (N, S, O), aromatic rings or long alkyl chains generally improves corrosion inhibition efficiency.

However, these organic compounds possess excellent corrosion inhibiting properties; the method of synthesis is expensive, tedious and toxic in nature. In sight of this, many alternative green corrosion inhibitors have now been developed. Al-Sahlanee *et al*.[8] found that Sesbania sesban extract can be used as good corrosion inhibitors for carbon steel in acidic medium. Recently, aqueous extracts of *Aleo vera*[9] and *Garlic extract*[10] and *Justicia gendarussa* plant[11] have been

reported to be efficient corrosion inhibitors for steel in acid solutions. Natural polymers have been investigated as a better inhibitor as they possess long chain molecules and show high inhibition efficiency at lower concentrations in corrosive media[12-14]. Literature reported that the synergistic effect of halide ions with natural polymer is effective corrosion inhibitors for metals in aggressive media[15]. But the synergistic effect between natural polymers and metal cations (Zn^{2+} and Ni^{2+}) towards the inhibition of corrosion is very limited.

Azadirachta indica gum (AI gum), a typical plant gum exudate is the salt of a complex polysaccharide acid[16]. It comprised of 35 % of proteinaceous materials and fatty acids. Thus, the complex structure of AI gum consisting of heteroatoms (N and O), suggests that it can be used as a potential material in several fields.

In the present work the corrosion inhibition of AI gum with metal cations (Zn^{2+} and Ni^{2+}) has been investigated by gravimetric, potentiodynamic polarization and electrochemical impedance spectroscopic methods. Temperature (303- 348 ± 1 K) and time (1, 2, 3, 4, 6 and 24 h) effect has also been studied and discussed in detail. Corrosion kinetic parameters and adsorption studies were carried out to find the nature of adsorption of the inhibitor on the metal surface. Further, Fourier transform infrared spectroscopy (FT-IR) was employed to examine the mode of inhibitor adsorption on the mild steel surface.

MATERIALS AND METHODS

The gum exudates of *Azadirachta indica A. Juss. Meliaceae* was collected locally and identified taxonomically and authenticated by the Botanical Survey of India (BSI), Coimbatore, Tamil Nadu, India. Zinc chloride and Nickel chloride used were analytical grade. Laboratory grade hydrochloric acid solution was used as an aggressive medium. All the solutions were prepared using double distilled water.

The mild steel of the composition 0.07 wt. % C, 0.008 wt. % P, 0.34 wt. % Mn, remaining iron (Fe) was used in the study. The metal specimens used for weight loss measurements were cut to obtain rectangular surfaces with dimensions of 25 x 10 x 1 mm with a hole drilled at the upper edge in order to hook it in the glass rod for immersion in the aggressive medium. Substantial layer of the specimen was removed by using various grades of abrasive papers and degreased by scrubbing with bleach- free scouring powder, followed by thorough rinsing in water and acetone.

The gravimetric experiments were carried out according to the ASTM practice standard G-31[17]. Before initiating the experiments, the pre-cleaned specimens were weighed on a balance using 0.1 mg precision. The weighed specimens were immersed in the corrosive medium with and without inhibitors for 1 hour. After the experiment, the specimens were removed from the corrosive medium and immersed in the clark solution for 40 seconds, rinsed with water, cleaned with acetone, dried in hot air and finally weighed. The mean of weight loss values of three identical specimens were used to calculate the corrosion rate and inhibition efficiency of the inhibitor. Corrosion rate and inhibition efficiency were calculated using the formulae given in equation (1) and (2)

$$\text{Corrosion rate (mmpy)} = 87.6 \times \frac{W}{\rho A t} \quad ...(1)$$

where, W is the weight loss (g), 'ñ' the density of the mild steel specimen (g cm^{-3}), 'A' the area of specimen (cm^2) and t is the time of exposure (h).

$$\text{Inhibition efficiency (\%)} = 1 - \frac{W_i}{W_o} \times 100 \quad ...(2)$$

where, W_i and W_o are the weight losses of mild steel in inhibited and uninhibited solution respectively.

The electrochemical experiments were performed using three-electrode cell assembly. The cell consisted of a platinum counter electrode and a saturated calomel electrode (SCE) as the reference electrode. The working electrode was immersed in the acid solution and the constant steady-state (open circuit) potential was recorded

as a function of time, when it became virtually constant. The polarization studies were carried out over a potential of + 200 to - 200 mV with respect to the open circuit potential at a scan rate of 1 mV s^{-1}. The linear Tafel segments of the cathodic curves and the calculated anodic Tafel lines were extrapolated to the point of intersection to obtain the corrosion potential (E_{corr}) and corrosion current density (I_{corr})[18]. The inhibition efficiency was evaluated from the measured I_{corr} values using equation (3)

$$\text{Inhibtion efficiency}(\%) = \frac{I^{o}_{corr} - I_{corr}}{I_{corr}} \times 100 \quad ...(3)$$

where, I^{o}_{corr} is the corrosion current density without inhibitor and I_{corr} is the corrosion current density with inhibitor.

The electrochemical impedance spectroscopic (EIS) measurements were carried out using AC signals of 10 mV amplitude over the frequency range of 10 KHz to 0.01 Hz. The electrode was immersed in the solution for half an hour before starting the impedance measurements. All the impedance data were automatically controlled by Z_{view} software and the diagrams were given as Nyquist plots. The charge transfer resistance (R_{ct}) values were obtained from the diameter of the semicircles of the Nyquist plots. The inhibition efficiency of the inhibitor has been found out from the charge transfer resistance values according to the following equation (4)

$$\text{Inhibition efficiency}(\%) = \frac{R_{ct} - R^{o}_{ct}}{R_{ct}} \times 100 \quad ...(4)$$

where, R_{ct} and R^{o}_{ct} are the charge transfer resistance with and without inhibitors respectively. To determine the interaction of inhibitors with the mild steel specimen, a Shimadzu FT- IR 8000 spectrophotometer is employed in the 4000-400 cm^{-1} region with KBr disc technique.

RESULTS AND DISCUSSION

Gravimetric measurements

The gravimetric measurements were carried out to calculate the corrosion rate and inhibition efficiency for the mild steel in 1 mol L^{-1} HCl in the absence and presence of different concentrations of Al gum with Zn^{2+} and Ni^{2+} separately for 1 h immersion period at 303 ± 1 K. The results of gravimetric studies using the binary systems (Al gum- metal cations) are shown in Table 1.

At lower concentrations, Al gum with metal cations shows very high corrosion rate with heavy mild steel dissolution. The corrosion rate decreases and the inhibition efficiency increases significantly by the addition of 0.06 g L^{-1} Al gum with Zn^{2+} (mixture A) and its efficiency reached upto 76.8 %. The inhibition efficiency of 81.2 % is obtained for the formulation consisting of 0.06 g L^{-1} Al gum - Ni^{2+} (mixture B). It is evident from the gravimetric results that mixture B shows better inhibition efficiency than mixture A.

Figure 1 represents the inhibition efficiency (%) as a function of different temperatures (303- 348± 1 K) for (a) 0.06 g L^{-1} Al gum; (b) 1 mmol L^{-1} Zn^{2+}; (c) 1 mmol L^{-1} Ni^{2+}; (d) mixture A and (e)

Table 1: Corrosion parameters for various concentrations of Al gum with metal cations on mild steel in 1 mol L^{-1} HCl

Concentration of Al gum (g L^{-1}) with 1 mmol L^{-1} of metal cations		Inhibition efficiency (%)		Corrosion rate × 10^{-2} (mmpy)		Synergism parameter (S_1)	
Zn^{2+}	Ni^{2+}						
0.02	0.02	56.4	62.7	3.43	3.09	1.59	1.57
0.04	0.04	58.1	69.6	3.32	2.56	1.58	1.44
0.06	0.06	76.8	81.2	1.85	1.51	1.24	1.28
0.08	0.08	75.4	78.0	2.64	1.73	1.43	1.32
0.1	0.1	69.2	76.2	3.55	1.96	1.64	1.30

mixture B. Analysis of Figure 1 (a) - (c) clearly shows that the decrease in inhibition efficiency with increase in temperature may be attributed to increase in the solubility of the protective films formed by the inhibitors[15]. In mixture A and B, the inhibition efficiency increase with increase in all the temperature range studied. The obtained inhibition efficiency at 348± 1 K for the mixture A and B are 88.4 % and 92.5 % respectively. From the results it is clear that the synergistic effect is more pronounced at elevated temperature than at lower temperature. Generally, increase in temperature changes the reaction rate. In the present study, not only the corroding rate of mild steel decreases but also the rate of synergistic effect between added metal cations and the Al gum increases. The results revealed that at high temperature synergistic effect predominates over dissolution of the mild steel. The increase in inhibition efficiency with increase in temperature is due to the specific interaction of mild steel surface with the inhibitors[19]. The increased inhibition efficiency with temperature was due to the change in the nature of adsorption mode, the inhibitor is being physically adsorbed at lower temperatures, while chemisorption is favored as temperature increases[20]. Thus, at high degree of surface coverage, the diffusion through the surface layer containing the inhibitor and corrosion products becomes the rate- determining step of the metal dissolution process[21].

To determine the corrosion inhibition stability of optimum concentration of Al gum, mixture A and B, the variation of inhibition efficiency with various immersion periods (1, 2, 3, 4, 5, 6 and 24 h) in 1 mol L^{-1} HCl was studied at 303± 1 K. The calculated values of inhibition efficiency are given in Table 2.

Table 2: Variation of inhibition efficiency with various immersion periods for mild steel in 1 mol L^{-1} HCl containing 0.06 g L^{-1}Al gum, mixture A and B

System	Inhibition efficiency (%)					
	1 h	2 h	3 h	4 h	6 h	24 h
Al gum	73.5	71.5	60.2	54.7	48.2	46.2
mixture A	76.8	78.9	71.7	72.8	71.9	82.4
mixture B	81.2	74.3	76.4	74.5	79.2.2	83.2

Table 3: Corrosion kinetic parameters for mild steel in 1 mol L-1 HCl in absence and presence of inhibitors

System	E^*_a(kJ mol^{-1})	ΔH*(kJ mol^{-1})	E^*_a-DH*(kJ mol^{-1})	ΔS*(J mol-1 K-1)
Blank	79.1	76.5	2.6	-32.0
0.06 g L^{-1} gum	94.4	91.7	2.7	6.95
1 mmol L^{-1} Zn^{2+}	91.0	88.4	2.6	4.34
1 mmol $L^{-1}$$Ni^{2+}$	98.8	96.2	2.6	27.8
mixture A	45.3	42.6	2.7	-148.2
mixture B	34.1	31.4	2.7	-184.7

Table 4: Adsorption parameters for mild steel in 1 mol L^{-1} HCl in the presence of various concentrations of Al gum with metal cations

Binary Systems	R^2	K_{ads} (M^{-1})	$\Delta G°_{ads}$(kJ mol-1)
Al gum- Zn^{2+}	0.9684	101.0	22.1
Al gum- Ni^{2+}	0.9981	156.2	23.0

Table 5: Potentiodynamic polarization parameters for the corrosion inhibition of mild steel in 1 mol L^{-1} HCl containing mixture A and B

System	I_{corr} (mA cm^{-2})× 10^{-4}	E_{corr} (mV/SCE)	b_a(mV dec^{-1})	b_c(mV dec^{-1})	Inhibition efficiency(%)
Blank	1.21	" 0.467	7.49	8.31	-
mixture A	0.49	" 0.459	8.37	6.92	58.6
mixture B	0.60	" 0.456	8.70	6.84	49.7

Table 6: Impedance parameters for mild steel in 1 mol L^{-1} HCl containing mixture A and B

System	R_{ct} (Ω cm^{-2})	R_s (Ω cm^{-2})	C_{dl} (μF cm^{-2})× 10^{-4}	Inhibition efficiency (%)
Blank	17.9	4.74	1.07	-
mixture A	30.1	4.67	0.52	41.0
mixture B	44.8	5.13	0.58	60.1

It is found that the inhibition efficiency increase with increase in immersion time period for mixture A and B and this may be attributed to the formation of an insoluble protective film on the surface of the mild steel[22]. The possible mechanism of inhibition action of an inhibitor is the adsorption of inhibitor onto the metal surface which blocks the metal surface and this do not permit the corrosion process to take place. Thus, the mixture A and B are proven to be a promising inhibitor that can be used even at higher temperatures and for longer immersion period.

Corrosion kinetic parameters

In an acidic solution the corrosion rate is related to temperature by Arrhenius equation

$$\log CR = \log A - \frac{E^*_a}{2.303RT} \quad ...(5)$$

where, 'CR' is the corrosion rate determined from the weight loss measurement, E^*_a is the apparent activation energy, 'A' the Arrhenius constant, 'R' the molar gas constant and *T* is the absolute temperature. The apparent activation energy is determined from the slopes of log (CR) versus 1/ *T* plot (Figure 2, 3) and their values are given in Table 3.

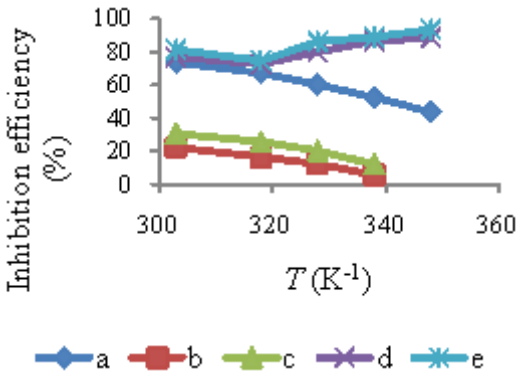

Fig. 1: Variation of inhibition efficiency against different temperatures for: (a) 0.06 g L^{-1} Al gum; (b) 1 mmol L^{-1} Zn^{2+}; (c) 1 mmol L^{-1} Ni^{2+}; (d) mixture A; (e) mixture B

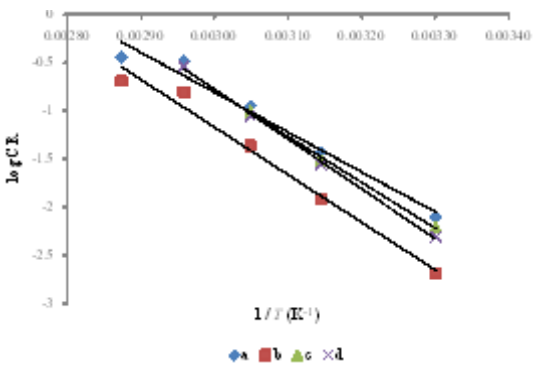

Fig. 2: Arrhenius plots for mild steel in 1 mol L^{-1} HCl. (a) blank; (b) 0.06 g L^{-1} Al gum; (c) 1 mmol L^{-1} Zn^{2+}; (c) 1 mmol L^{-1} Ni^{2+}.

It is seen that E^*_a values obtained for Al gum and metal cations (individually) are higher than blank, indicating a strong inhibitive action of inhibitors by increasing energy barrier for the corrosion process, emphasizing the electrostatic interaction (physisorption) between the mild steel surface and the inhibitors. On contrary to this, lower values of obtained for the corrosive medium containing the mixture A and B attributes to chemisorption[23]. The decrease in at higher level of inhibition arises due to a shift of the net corrosion reaction from that on the uncovered surface to one involving the adsorbed sites directly[24,25].

The change of enthalpy (ΔH*) and entropy (ΔS*) for the corrosion process in 1 mol L^{-1} HCl in the presence of Al gum, metal cations and mixture A, B were obtained by the equation (6)

$$CR = \left(\frac{RT}{Nh}\right)\exp\left(\frac{\Delta S^*}{R}\right)\exp\left(\frac{-\Delta H^*}{RT}\right) \quad ...(6)$$

where, h is Planck's constant, 'N' the Avogadro's number, R is the universal gas constant, '*T*' the absolute temperature. Figure 4 and 5 shows the plot of log (CR/ *T*) versus 1/ *T*, gives straight line with slope (-ΔH*/ 2.303 R) and an intercept (log (R/ Nh) + ΔS*/ 2.303 R), from which ΔH* and ΔS*are calculated and the values are included in Table 3. The enthalpy change of Al gum and metal cations

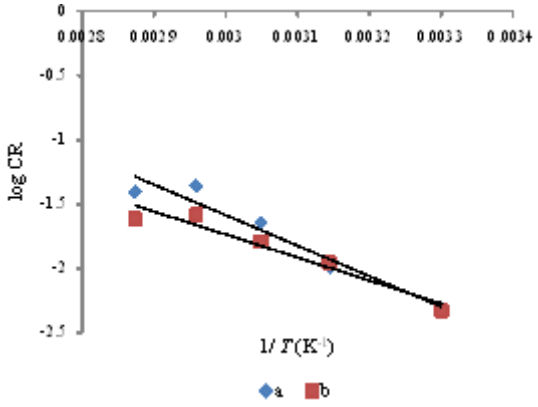

Fig. 3: Arrhenius plots for mild steel in 1 mol L^{-1} HCl in the presence of: (a) mixture A;(b) mixture B

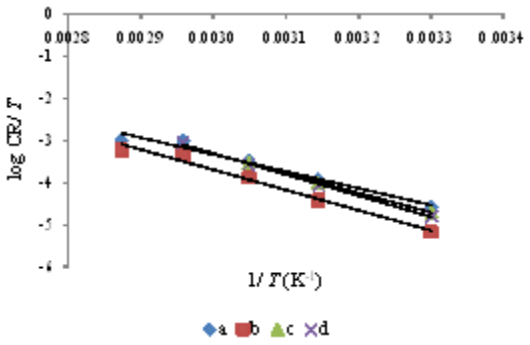

Fig. 4: Transition state plots for mild steel in 1 mol L^{-1} HCl. (a) blank; (b) 0.06 g L^{-1} Al gum; (c) 1 mmol L^{-1} Zn^{2+}; (d) 1 mmol L^{-1} Ni^{2+}

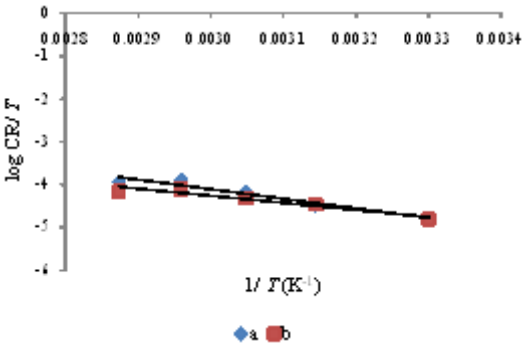

Fig. 5: Transition state plots for mild steel in 1 mol L^{-1} HCl in the presence of: (a) mixture A; (b) mixture B

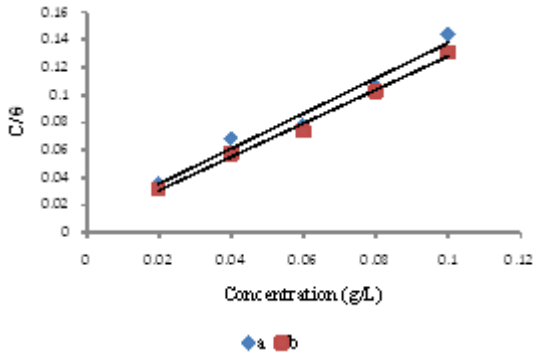

Fig. 6: Langmuir adsorption isotherm plots for mild steel in 1 mol L^{-1} HCl. (a) Al gum- Zn^{2+} system; (b) Al gum- Ni^{2+} system

(individually) are greater than the plain acid correspond to physisorption[24]. But in the case of mixture A and B, the ΔH* values are lower than the blank, again supports chemical mode of adsorption. We also noted that and values vary in the same way for all the systems studied. From the kinetic studies, the unimolecular reactions are characterized by following equation

$$E_a^* - \Delta H^* = RT \quad \text{... (7)}$$

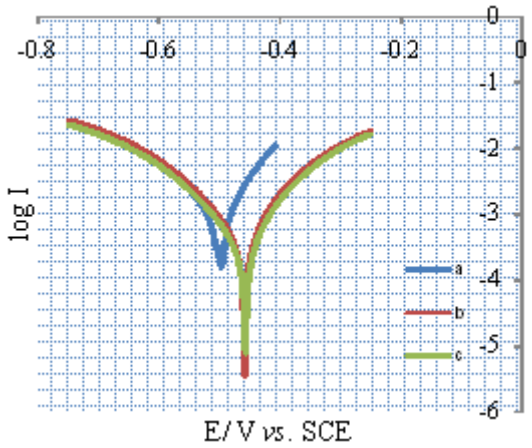

Fig. 7: Potentiodynamic polarization curves for mild steel in 1 mol L^{-1} HCl. (a) blank; (b) mixture A; (d) mixture B

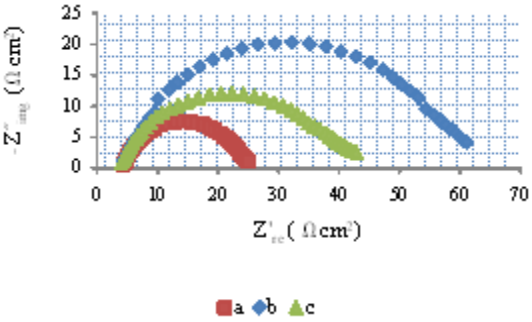

Fig. 8: Nyquist plots for mild steel in 1 mol L^{-1} HCl. (a) blank; (b) mixture A; (c) mixture B

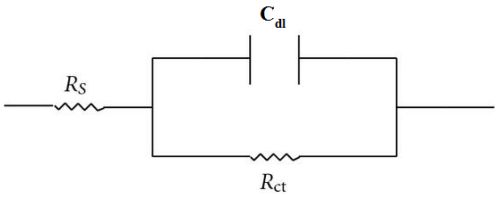

Fig. 9: Electric circuit used to simulate EIS data

The calculated values are too close to RT (2.67 kJ mol^{-1}). This result shows that inhibitors acted equally on E^*_a and ΔH*.

The positive values of ΔS* for the inhibited systems containing 0.06 g L^{-1} Al gum and metal cations (individually) shows that an increase in disordering takes place on going from reactant to the activated complex[26]. The behavior of individual inhibitors in the corrosive medium can be explained by the fact that on adding Al gum and metal cations individually to the aggressive medium, the inhibitor molecules move freely in the bulk solution, this results in increase in disorderliness of the system. The negative values of ΔS* for the mixture A and B imply that the activation complex in the rate determining step represents association meaning that a decrease in disordering takes place on going from reactants to the metal/solution interface[24]. This is the driving force for the adsorption of inhibitors onto the mild steel surface.

Synergism parameter

All the experimental results have suggested that the addition of metal cations to the Al gum increases the inhibition efficiency. The enhanced inhibition behavior is attributed to the synergism existing between the Al gum and metal cations. The extent of synergistic effect exhibited by the inhibitor mixture A and B has been analyzed by evaluating the synergism parameter (S_1) obtained from the gravimetric measurements[27].

$$S_1 = \frac{1 - \eta_{1+2}}{1 - \eta'_{1+2}} \quad \text{...(8)}$$

where, $\bullet_{1+2} = \bullet_1 + \bullet_2$; $\bullet_1$ = inhibition efficiency of Al gum; $\bullet_2$ = inhibition efficiency of metal cations and $\bullet^1$ = measured inhibition efficiency for the inhibitor mixture. The calculated values of S_1 are included in Table 1. Analysis of Table 1 reveals that the S_1 values are greater than unity suggesting the synergistic action of metal cations with Al gum. The observed synergistic effect exhibited by the inhibitor mixture A and B may be due to the co-adsorption of the Al gum and the metal cations on the mild steel surface in 1 mol L^{-1} HCl.

Adsorption considerations

It is very essential to define empirically which adsorption isotherm fits best to the surface coverage data in edict to calculate the thermodynamics parameters pertaining to inhibitor adsorption on the mild steel surface[28]. The adsorption provides information about the adsorbed molecules as well as their interaction with the metal surface. The surface coverage (¸) of the inhibitors at different concentrations is used to obtain the best adsorption isotherm. ¸ values have been calculated using the following relationship

$$\theta = 1 - \frac{W_i}{W} \quad ...(9)$$

Various adsorption isotherms like Langmuir, Freundlich, Temkin, El- Awady *et al*. were tested. The experimental data fit best for the Langmuir adsorption isotherm and it is given by the following equation

$$\frac{C}{\theta} = \frac{1}{K_{ads}} + C \quad ...(10)$$

where, C is the concentration, θ is the degree of surface coverage and K_{ads} is the equilibrium constant for the process of adsorption. Figure 6 represents the Langmuir adsorption isotherm for binary systems with slopes of unity. From the intercept of the straight lines, K_{ads} values are obtained and their values are given in Table 4.

Large values of K_{ads} indicate that there is a strong interaction between the phase boundaries of double layer and the adsorbed inhibitor mixtures, which results in better inhibition efficiency. The equilibrium constant of adsorption K_{ads} is related to the standard free energy of adsorption ($\Delta G°_{ads}$ ΔG^{o}_{ads}) by:

$$K_{ads} = \frac{1}{55.5} \exp\left(\frac{-\Delta G^{o}_{ads}}{RT}\right) \quad ...(11)$$

The value 55.5 in the equation is the molar concentration of water molecules at electrode/ electrolyte interface. The standard free energy of adsorption ($\Delta G°_{ads}$) can be calculated by using the above equation. The negative values of ensure the spontaneity of the adsorption process and stability of the adsorbed layer on the steel surface (Table 4). Generally, values of $\Delta G°_{ads}$ up to Δ20 kJ mol^{-1} are consistent with electrostatic interactions between the charged molecules and the metal (physisorption) while those around Δ40 kJ mol^{-1} or higher are associated with chemisorption as a result of sharing or transfer of electrons from organic molecules to the metal surface to form a coordinate type of bond. In the present work, the values of $\Delta G°_{ads}$ obtained are less positive than Δ40 kJ mol^{-1} and more negative than Δ20 kJ mol^{-1} clearly indicate that the adsorption process is not merely physisorption or chemisorption but obeying a comprehensive adsorption (physisorption and chemisorption).

Electrochemical measurements

Figure 7 shows the polarization curves for mild steel in 1 mol L^{-1} HCl with and without mixture A and B at 303 ± 1 K. The addition of mixtures into the acid solution affects both the anodic and cathodic curves to lower current densities, while corrosion potential (E_{corr}) is only slightly shifted. This implies that mixture A and B functions as a mixed-type inhibitor. The cathodic and anodic current potential curves are extrapolated to obtain the values of corrosion current (I_{corr}) and corrosion potential (E_{corr}). The electrochemical parameters I_{corr}, E_{corr}, anodic and cathodic Tafel slopes (b_a, b_c) obtained from polarization data and listed in Table 5.

It is evident from the table that I_{corr} decreases considerably, indicating an inhibiting effect of the Al gum with metal cations. Also, there is no pronounced change observed in the anodic and cathodic Tafel slopes, suggesting that the inhibitors adsorbs onto the mild steel surface and prevent it from corrosion by blocking the active sites without altering the anodic and cathodic reaction mechanism[29]. The observed inhibition efficiency values obtained are in good agreement with those determined from weight loss measurements.

Synergistic effects are also revealed in the impedance spectra obtained for mild steel in 1 mol L^{-1} HCl in the presence of mixture A and B at 303 ± 1 K. The impedance spectra of the Nyquist plot are

shown in Figure 8. It describes a single, capacitive-like depressed semi-circle with their centres in the real axis and with their diameters increasing on the addition of mixture A and B to the corrosive medium. The single semicircle indicates that the corrosion process is charge transfer control from the mild steel to the corrosive medium through the electrochemical double layer. The real axis intercepts at high and low frequencies are bigger in the presence of mixture A and B, which means that the impedance of the mild steel in the inhibited solutions is greater than the uninhibited solution[30].

EIS data can be calculated by using equivalent electric circuit model, which is depicted in Figure 9, which includes the solution resistance

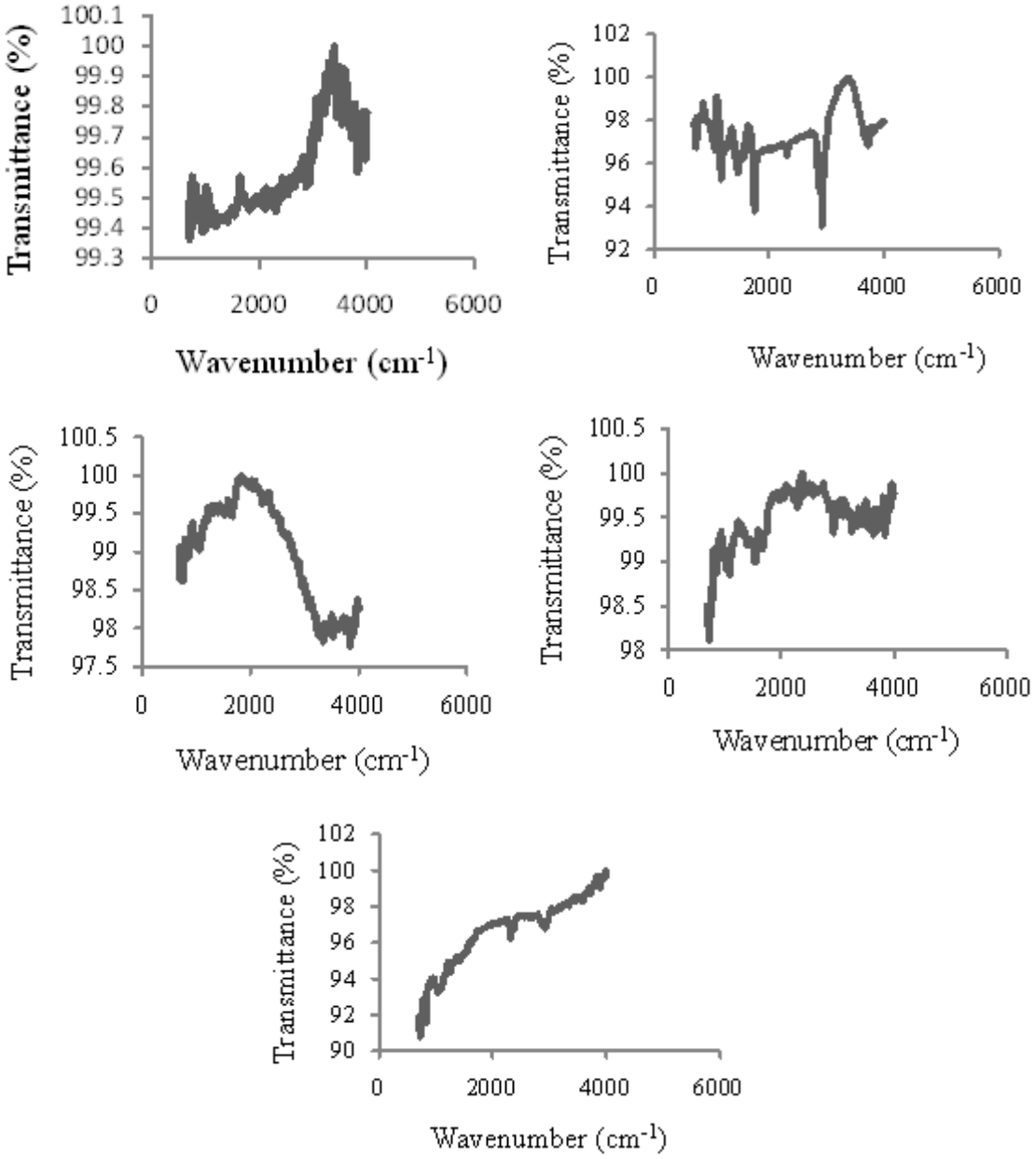

Fig. 10: FT- IR spectrum of: (a) Pure Al gum; (b) Mild steel specimen immersed in the presence of 0.06 g L^{-1} Al gum; (c) mixture A at 303± 1 K; (d) mixture B at 303 ± 1 K; (e) mixture B at 348± 1 K

R_s and the double layer capacitance C_{dl} which is placed in parallel to the charge transfer resistance $R_{ct.}$ The R_{ct} values were calculated from the difference in impedance at low and high frequencies[31]. The value of R_{ct} is a measure of electron transfer across the surface and inversely proportional to corrosion rate. Double layer capacitance (C_{dl}) was obtained from the impedance measurements by using equation (12)

$$C_{dl} = \frac{1}{2\pi f_{max} R_{ct}} \quad ...(12)$$

where, f_{max} is the frequency value at which the imaginary component of the impedance is maximum. The values of R_{ct}, C_{dl} and inhibition efficiency for mild steel in 1 mol L^{-1} HCl for mixture A and B are given in Table 6.

It is important to note that by the addition of mixture A and B to the corrosive medium brings as increase in the R_{ct} values and a decrease in C_{dl} values with increase in the percentage of inhibition efficiency. The decrease in C_{dl} values are due to the replacement of water molecules by the adsorption of inhibitor mixture, resulting in the formation of protective film on the mild steel surface and decrease the corrosion rate[32].

FT-IR spectra

FT-IR spectrum of pure Al gum is shown in Figure 10 (a). The characteristic bands in the region between 3317 cm^{-1} – 3618 cm^{-1} are assigned to the – OH stretching vibration and another peak at 1658 cm^{-1} is due to bending mode of water molecules[33]. The – C=O stretching frequency is seen at 1705 cm^{-1}. The asymmetric stretching vibration frequency of - COO^- and – C-O stretching frequency[34] are seen at 1550 cm^{-1} and 1080 cm^{-1} respectively. In the spectrum of mild steel in 1 mol L^{-1} HCl in the presence of Al gum (Figure 10 (b)), the intensity of – OH stretching frequency is shifted in the region between 3309 cm^{-1} – 3664 cm^{-1}, the – C=O peak on contrary are seen to be shifted towards higher wave number (1743 cm^{-1}). The peak for bending mode of H_2O molecule is disappeared. The asymmetric stretching frequency of – COO^- is shifted from 1550 cm^{-1} to 1535 cm^{-1}. The above shifting in the characteristic peaks clearly indicates that the Al gum adsorbed on to the mild steel surface through lone pair of electrons of oxygen atom of – COO^- ions.

Figure 10 (c) and (d) represents the FT-IR spectra of mild steel specimen immersed in 1 mol L^{-1} HCl at 303± 1 K in the presence of mixture A and B respectively. The – OH stretching frequency bands are shifted towards higher wave numbers in both the spectrum. The bending mode of H_2O molecule is shifted towards lower frequency side of 1620 cm^{-1} and 1627 cm^{-1} in mixture A and B respectively. This clearly indicates that metal cations (Zn^{2+} and Ni^{2+}) in corrosive medium, may reacts with – OH group of Al gum forming insoluble hydroxides, protecting the mild steel surface from the corrosive attack. In addition to that the asymmetric stretching frequency of – COO^- anions is shifted towards lower side of 1512 cm^{-1} for mixture A and 1519 cm^{-1} for mixture B. This lower side shifting shows that the – COO^- anions of Al gum makes possible its adsorption by co-ordinate type linkage through transfer of lone pairs of electron of oxygen atoms to the metal cations (Zn^{2+} and Ni^{2+}), giving a stable chelate. The simultaneous interaction of metal cations with Al gum, make it horizontally oriented at the mild steel surface, which led to increase the surface coverage, resulting in increase in the inhibition efficiency.

To verify the stability of the protective layer formed by Al gum- metal cations at higher temperatures, FT-IR spectrum of mild steel in 1 mol L^{-1} HCl in the presence of mixture B at 348± 1 K was recorded (Figure 10(e)). On comparing this spectrum with Figure 10 (d), the characteristic stretching frequency of bending mode of water molecules doesn't experiences a change when temperature increases. The – COO^- anions peak is shifted towards lower side of 1504 cm^{-1}.It indicates that at higher temperatures more Ni^{2+} cations co-ordinated with – COO^- anions of Al gum, makes the protective film more stronger.

Thus, it is evident from FT- IR studies that the protective film formed on the mild steel surface did not show any significant change during higher temperature (348 ± 1 K), forms a evidence for a distinctive comprehensive adsorption mechanism followed by mixture A and B.

CONCLUSION

Synergistic effect between AI gum and metal cations have been observed from the weight loss measurements and acting as an effective inhibitor for the corrosion of mild steel in 1 mol L^{-1} HCl. The synergistic influence of Ni^{2+} cation in AI gum is more pronounced than Zn^{2+} ion. Increase in temperature causes increase in inhibition efficiency for both the mixture. Additionally, the decrease in apparent activation energy in the mixture A and B supports the chemical mode of adsorption of inhibitors on the mild steel surface. It obeys Langmuir adsorption isotherm. According to the ΔG°_{ads} values, spontaneous and comprehensive adsorption of inhibitor mixtures is suggested to occur on the mild steel surface. A mixed- inhibition mechanism is proposed from the potentiodymanic polarization studies. It can also be concluded from FT-IR studies, the metal cations are preferentially adsorbed on the mild steel surface by columbic attraction where – COO^{-} anions of the AI gum is already chemisorbed and suppresses the corrosion rate by the stabilization of adsorbed anion and by increase in inhibition efficiency

REFERENCES

1. Banerjee, S.; Srivastava, V.; Singh, M. M. *Corros. Sci*. **2012**, *59*, 35–41.
2. Guo, W.; Chen, S.; Feng, Y.; Yang, C. *J. Phys. Chem. C*. **2007**, *111*, 3109–3115.
3. Zaafarany, I. A. *Int. J. Electrochem. Sci*. **2013**, *8*, 9531- 9542.
4. Singh, M. M.; Rastogi, R. B.; Upadhyay, B. N.; Yadav, M. *Ind. J. Chem. Tech*. **2003**, *10*, 414.
5. Ashassi- Sorkhabi, H.; Seifzadeh, D.; Hassanein, M. G. *Corros. Sci*. **2008**, *50*, 3363-3370.
6. Shaju, K.S.; Joby thomas, K.; Raphael. V.P. *Orient J Chem.***2014,** *30***,** 807-813
7. Oguzie, E. E.; Wang, S. G.; Li, Y.; Wang, F. H. *J. Phys. Chem. C.* **2009**, *113*, 8420.
8. Al-Sahlanee, H.H.; Sultan, A.A. *Aqua. Sci. Tech*. **2013**, *1*, 135-151.
9. Abiola,O.K.; James, A.O. *Corros. Sci*. **2010**, *52*, 661-664.
10. Al-Mhyawi. S.R. *Orient J Chem.***2014,** *30,* 541-552.
11. Satapathy, A.K.; Gunasekaran, G.; Sahoo, S.C.; Amit, K.; Rodrigues, P. V. *Corros. Sci*. **2009**, *51*, 2848-2856.
12. Zaafarany, I. *Port. Electrochim. Acta.* **2012,** *30*, 419-426.
13. Abdallah, M. *Port. Electrochim. Acta.* **2004**, *22*, 161-175.
14. Umoren, S.A.; Obot, I.B.; Ebenso, E.E.; Obi-Egbedi, N.O. *Int. J. Electrochem. Sci.* **2008**, *3*, 1029-1043.
15. Umoren, S.A.; Ebenso, E.E. *Mater. Chem. Phy.* **2007**, *106*, 387-393.
16. Mukerjee, S.; Srivastava, H.C. *J. Am. Chem. Soc.* ***1955****, 77*, 422-423.
17. ASTM practice standard G-31 "Standard practice for laboratory immersion corrosion testing of metals", ASTM International, 2004.
18. McCafferty, E. *Corros. Sci*. **2005**, *47*, 3202-3215.
19. Ammar, I.A.; El Khorafi, F.M. *Werkst. Korros*. **1973**, *24*, 702-707.
20. Ivanov ES. Inhibitors for Metal Corrosion in Acidic Media. Metallurgy, Moscow; 1986.
21. Bouklah, M. Hammouti, B.; Lagrenee, M.; Bentiss, F. *Corros. Sci.* **2006**, *48*, 2831-2842.
22. Granese, S.L.; Rosales, B.M.; Ociede, C.; Zerbino, J.O. *Corros. Sci.* **1992**, *33*, 1439-1453.
23. Umoren, S.A.; Solomon, M.M.; Udosoro, I.I.; Udoh, A.P. *Cellulose.* **2010**, *17*, 635-648.
24. Riggs, O.L.; Hurd, R.M. *Corrosion*. **1967**, *23*, 252-258.
25. Ehteram, A. Noor.; Aisha H. Al-Moubaraki. *Mater. Chem. Phys.* **2008,** *110*, 145-154.
26. Mingcan, C.; Min, J.; Sang Hyun, C.; Jeehyeong, K. *Environment. Tech.* **2010**, *31*, 1203-1211.
27. Aramaki, K.; Hackerman, N. *J. Electrochem. Soc.* **1969**, *116*, 568-574.
28. Obi-Egbedi, N.O.; Essien, K.E.; Obot, I.B. *J. Comput. Method. Mol. Design.* **2011**, *1*, 26-

43.
29. Helal , N.H. *J. Chem. Engg. Mater. Sci.* **2011**, *2*, 28-38.
30. Valle- Quintana, J.C.; Dominguez-Patino, G.F.; Gonzalez- Rodriguez, J.G. *Int. J. Corros.* **2014**, Article ID 945645, 8 pages.
31. Amin, M.A.; Khaled, K.F.; Fadl- Allah, S.A. *Corros. Sci.* **2010**, *52*, 140-151.
32. Elewady, G.Y. *Int . J. Electrochem. Sci.* **2008,** *3*, 1149-1161.
33. Andreeva, D.V.; Skorb, E.V.; Shchukin, D.G. *App. Mater. Interfaces.* **2010**, *2*, 1954.
34. Silverstein RM, Bassler GC, Morill TC. Spectrometric identification of organic compounds. Wiley: New York, USA, (1978).